Development of cysteamine loaded liposomes in liquid and dried forms for improvement of cysteamine stability

Carla Atallah, Hélène Greige-Gerges, Catherine Charcosset

Development of cysteamine loaded liposomes in liquid and dried forms for improvement of cysteamine stability

Carla Atallah[a,b], Hélène Greige-Gerges[a], and Catherine Charcosset*[b]

[a]*Bioactive Molecules Research Laboratory, Faculty of Sciences, Lebanese University, Lebanon*

[b]*Laboratoire d'Automatique, de Génie des Procédés et de Génie Pharmaceutique (LAGEPP), Université Claude Bernard Lyon 1, France.*

***Corresponding Author:**
Claude Bernard Lyon 1 University
Laboratory of Automatic Control, Chemical and Pharmaceutical Engineering
308 G Bldg., CPE
43 Bd du 11 Novembre 1918
69 622 Villeurbanne Cedex, France
Tel: 04 72 43 18 34
Fax: 04 72 43 16 99
E-mail : catherine.charcosset@univ-lyon1.fr

Abstract

Despite the high aqueous solubility of cysteamine, its unpleasant organoleptic properties, hygroscopicity, instability in solutions, and poor pharmacokinetic profile are the main drawbacks that limit its use for medical and cosmetic purposes. In this study, cysteamine-loaded liposomes were prepared using the ethanol injection method. Liposomes were characterized for their size, homogeneity, surface charge, and morphology. The incorporation ratios of cholesterol and phospholipids, the encapsulation efficiency and the loading ratio of cysteamine in liposomes were determined. Moreover, the stability of free and encapsulated cysteamine was assessed at different temperatures (4, 25, and 37°C) in the presence and absence of light. Cysteamine-loaded liposomes were freeze-dried and reconstituted liposomes were characterized. Finally, the storage stability of the freeze-dried cysteamine-loaded liposomes was studied. Liposomes were nanometric, oligolamellar, and spherical. The encapsulation efficiency and the loading ratio of cysteamine varied between 12 and 40% in the different formulations. The encapsulation improved the stability of cysteamine in the various storage conditions. The dried form of cysteamine-loaded liposomes conserved the size of the vesicles and retained 33% of cysteamine present in the liposomal suspension before lyophilization. The freeze-dried liposomes formulations were stable after four months of storage at 4°C.

Keywords: Cysteamine; Encapsulation; Freeze-drying; Liposomes; Stability.

1. Introduction

Cysteamine (Cyst) is an aminothiol compound synthesized by human body cells and derives from coenzyme A degradation (Besouw et al., 2013; Gallego-Villar et al., 2017) (**Fig. 1**). Cyst is described to have a radioprotective (Bacq et al., 1953), an anti-cancer (Apffel et al., 1975), and anti-malarial (Min-Oo et al., 2010) effects. It can be used for hyperprolactinemia treatment by reducing the size of pituitary glands and depleting plasma prolactin (Sagar et al., 1985). This molecule represents the only treatment of cystinosis disease, which is characterized by cystine accumulation in many tissues (Elmonem et al., 2016). In lysosomes, cysteamine reacts with cystine to form a mixed disulfide of half-cystine and Cyst, which then leaves the cells via a lysine transporter (Bozdağ et al., 2008). It can also be used as a depigmenting agent (Chavin and Schlesinger, 1966; Farshi et al., 2018; Frenk et al., 1968; Mansouri et al., 2015). Cyst is freely soluble in water (23.5 mg/mL), has a foul odor and a bitter taste, and presents a weak pharmacokinetic profile (Lahiani-Skiba et al., 2007). Besides, Cyst is unstable in aqueous solutions due to the rapid oxidation of the sulfhydryl group, leading to the formation of cystamine. This reaction is catalyzed by metal ions such as Cu^{2+}, Fe^{3+}, and Zn^{2+} and is stimulated in alkaline pH (Atallah et al., 2020). To increase its stability and improve its biological effects, Cyst has been encapsulated in liposomes (Butler et al., 1978; Jaskierowicz et al., 1985; Jeitner and Oliver, 1990), cyclodextrins (Lahiani-Skiba et al., 2007), and emulsions (Gresham et al., 1971).

Liposomes are spherical vesicles that comprise one or more lipid bilayer structures enclosing an aqueous core. They are used to encapsulate active compounds for various applications (Laouini et al., 2012). Their biocompatibility, biodegradability, and low toxicity make them very appropriate carriers for many drugs (Zylberberg and Matosevic, 2016). Cyst has been encapsulated in liposomes to enhance its absorption through the intestinal wall (Butler et al., 1978), its effectiveness in cystinosis (Jaskierowicz et al., 1985), and the period of prolactin depletion action (Jeitner and Oliver, 1990). To the best of our knowledge, the liposomes

encapsulating Cyst were not characterized in previous studies, and the effect of encapsulation on Cyst stability was not evaluated.

The freeze-drying is a promising approach to increase the shelf life of liposomes incorporating active agents. Among several cryoprotectants (sucrose, trehalose, glucidex 6D and 19D), *Sebaaly et al.* demonstrated that hydroxypropyl beta-cyclodextrin (HP-β-CD) was the most effective cryoprotectant of liposomes during the freeze-drying of eugenol-loaded Phospholipon 90H (PH 90H) liposomes (Sebaaly et al., 2016). Besides, *Gharib et al.* proved that HP-β-CD protects hydrogenated but not unsaturated liposomes during freeze-drying (Gharib et al., 2018).

In this study, blank and Cyst-loaded liposomes composed of PH 90H and Lipoid S100 were prepared by the ethanol injection method. The liposomal suspensions were characterized for their size, polydispersity index (PdI), and zeta potential by diffusion light scattering (DLS) as well as for their morphology using transmission electron microscopy (TEM). The concentrations of Cyst, phospholipid, and cholesterol (Chol) in liposomes were determined spectrophotometrically by the Ellman method with some modifications, Bartlett method and Chol quantitation kit, respectively. The encapsulation efficiency (EE%) and the loading ratio (LR %) of Cyst in liposomes were also determined. Freeze-drying of PH 90H liposomes was realized according to the optimized protocol previously described (Gharib et al., 2018), and the characteristics of the reconstituted vesicles were determined. Moreover, the stability of free and encapsulated Cyst was assessed at different temperatures (4, 25, and 37°C) and in the presence and absence of room light. Finally, the storage stability of the freeze-dried form of encapsulated Cyst was evaluated after four months of storage at 4°C.

2. Materials and methods

2.1 Materials

Cyst, monobasic phosphate, cystamine dihydrochloride, DL-dithiothreitol, and metformin hydrochloride were purchased from Sigma-Aldrich (Buchs, Switzerland). 5,5′- Dithiobis(2-nitrobenzoic acid) (DTNB), ammonium molybdate were purchased from Sigma-Aldrich (St Louis, Missouri, USA). Ethylenediaminetetraacetic acid (EDTA), dibasic phosphate, sulfuric acid, and hydrogen peroxide were purchased from Sigma-Aldrich (Steinheim, Germany). PH 90 H (90% soybean PC, 4% lysoPC, 2% triglycerides, 2% water, and 0.5% ethanol) and Lipoid S100 (94% soybean PC, 3% lysoPC, 0.5% N-acyl-PE, 0.1% PE, 0.1% phosphatidylinositol, 2% water, 0.2% ethanol) were obtained from Lipoid GmbH (Ludwigshafen, Germany). Chol was obtained from the Fisher chemical (Loughborough, UK), and sodium bisulfite was purchased from Combi Blocks (San Diego, California, USA). 4-Amino-3-hydroxy-1-naphthalene sulfonic acid was purchased from Sigma-Aldrich (Bangalore, India). Chol quantitation kit was purchased from SPINREACT (Barcelona, Spain). HP-β-CD-oral grade (MS=0.85) was purchased from Roquette (Lestrem, France). Sodium dodecyl phosphate and phosphoric acid were obtained from Sigma-Aldrich (China). All other chemicals were of analytical grade.

2.2 Cyst quantification

The quantification of Cyst was done using two methods. For the quantification of Cyst in liposomal suspension, a modified Ellman method was used. First, a stock solution of Cyst was prepared in water (1 mg/mL) and then diluted to obtain final concentrations of Cyst ranging between 2.5 and 100 µg/mL. Ellman's reagent was prepared by dissolving 4 mg DTNB in 1 mL of reaction buffer (pH 8.0). The latter is composed of 0.1 M sodium phosphate and 1 mM EDTA. 250 µL of water (blank) or Cyst solution was added to 1.25 mL reaction buffer, 1.25 mL of methanol, and 50 µL Ellman's reagent solution. This reaction mixture was then

vortexed and incubated at room temperature for 15 min. The absorbance was measured at 412 nm using the Spectrophotometer UV5 Mettler Toledo (Columbus Ohio, USA). The calibration curve was constructed by plotting the absorbance against the concentration of Cyst ranging from 2.5 to 100 µg/mL.

For the stability studies, the simultaneous quantification of Cyst and its degradation product cystamine was needed. An ion-pair chromatography with an isocratic mode consisting of acetonitrile: water containing 0.1% phosphoric acid and SDS (4 mM) (v/v, 45:55) was used. 20 µL of the samples were injected into a reverse-phase Kinetex C18 column (4.6 × 100 mm, 2.6 µm). The flow rate was set at 1.0 mL/min, the column temperature was maintained at 25°C, and the detection wavelength was 215 nm. Metformin was used as an internal standard with a concentration of 1 µg/mL. Linearity was between 2.5 and 100 µg/mL for Cyst and between 5 and 100 µg/mL for cystamine.

2.3 Preparation of liposomes

Liposomes were prepared by the ethanol injection method, as described by Sebaaly et al. (2016). Saturated (PH 90H) or unsaturated lipids (Lipoid S100) (10 mg/mL) and Chol (5 mg/mL) were dissolved in absolute ethanol to obtain the organic phase (10 mL). Then, the organic phase was injected into the aqueous phase (20 mL) containing different concentrations of Cyst (0; 0.5; 0.75; 1; 2.5; 5 mg/mL), using a syringe pump (Fortuna optima, GmbH-Germany), at a temperature above the transition temperature of the phospholipid (55°C for PH 90H and -20°C for Lipoid S100) and under magnetic stirring at 400 rpm. The phospholipid:Chol:Cyst molar ratios ranged between 1:0.98:1 and 1:0.98:10; for PH 90H and between 1:1.17:1.17 and 1:1.17:11.7 for Lipoid S100. The contact between the organic solution and the aqueous phase leads to a spontaneous liposome formation. The liposomal suspensions were then left for 15 min at 25 °C under stirring (400 rpm). The ethanol was removed by rotary evaporation (Heidolph GmbH, Germany) under reduced pressure at 40 °C

and the obtained liposomal solutions were stored at 4 °C for further characterization. Each preparation was performed in triplicate.

2.4 Characterization of the liposomal suspensions

2.4.1 Determination of size, pdI and zeta potential by dynamic light scattering

Malvern Zetasizer Nanoseries (Zetasizer Nano ZS; Malvern Instruments Ltd, France) was used to determine the mean size of the vesicles. All batches were diluted with ultrapure water. The particle-size distribution data were collected using the DTS (nano) software (version 5.10) provided with the instrument. The polydispersity index, which indicates the particle size distribution, ranges from 0 (monodispersed) to 1 (very broad distribution). Zeta potential was calculated using Smoluchowski's equation from the electrophoretic mobility of liposomes. All measurements were carried out at 25°C after 2 min of equilibration and were performed in triplicate. Data were expressed as the mean values ± SD.

2.4.2 Morphological characterization by transmission electron microscopy

The morphology of the liposomal suspensions was imaged by transmission electron microscope (TEM) (CM 120; Philips, Eindhoven, Netherlands) operating at an accelerating voltage of 120 kV. A drop of a solution of the liposomal suspension with or without dilution was placed onto a carbon-coated copper grid for 2 min, and the remaining liquid was removed using a filter paper. The grid was placed on negative staining using a 1% sodium silico-tungstate solution during 30 s. The excess amount of sodium silicotungstate solution was removed using a filter paper, and dried samples were observed.

2.4.3 Determination of phospholipid:Chol:Cyst molar ratios in the final liposome structures

The concentrations of incorporated compounds (phospholipids, Chol, and Cyst) in lipid vesicles were obtained by subtracting the concentrations of free compounds from their total concentrations determined in the suspensions. The suspensions underwent centrifugation at

21382xg during 1 h at 4°C using Vivaspin 500 centrifugal concentrator (Sartorius Stedim Biotech, Germany, MWCO = 10 kDa). The filtrates contained the free compounds.

2.4.4 Phospholipid quantification assay

Bartlett's method was used to determine free and total concentrations of phospholipids in the various liposomal suspensions. This method is based on several steps; first, the digestion of the organic phosphate (0.5 mL from total liposomal suspensions, filtrates, and standard solutions of phosphorus) using diluted sulfuric acid (5 mM) at 200°C for 1h. Then, the oxidation to the inorganic phosphates was done in the presence of 10% hydrogen peroxide (0.1 mL) for 30 min at 200°C. A phosphomolybdic complex was formed after the addition of ammonium molybdate (4.6 mL) and the reduction of this complex by the 4-amino-3-hydroxyl-1-naphthalene sulfonic acid (0.2 mL) at 100°C for 15 min. A blue solution appeared and was measurable at 815 nm spectrophotometrically.

The incorporation ratio (IR) of phospholipids was calculated as follows:

$$\text{IR } \% = \frac{\text{Incorporated mass of phospholipids}}{\text{Initial added mass of phospholipids}} \times 100 \quad \text{Eq. (1)}$$

where the incorporated mass of phospholipids stands for the phospholipid mass determined in the liposome structure; the initial mass of phospholipids represents the mass initially used to prepare liposomes.

2.4.5 Chol quantification assay

The quantification of Chol (free form or total amount present in the suspension) was performed after its enzymatic hydrolysis and oxidation using the Chol CHOD-POD kit (SPINREACT, Spain). Chol in the samples was oxidized by Chol oxidase into 4-cholestenona and hydrogen peroxide. The latter reacts with 4-aminophenazone in the presence of peroxidase to form the colorimetric indicator quinonimine, having an absorbance proportional to Chol concentration in the sample. Standard solutions (0 to 2 mg/mL) were prepared from

Chol stock solution (2 mg/mL); the latter was prepared in 10% Triton X-100. Samples from the liposome suspensions were diluted in 10% Triton X-100 and sonicated for 20 min at room temperature to ensure the dissolution of vesicles and the release of incorporated Chol. 1 mL of the working reagent containing buffer and enzyme was then added to 10 µL of each sample (liposome suspension, filtrate, and Chol standard solution) and incubated for 10 min at room temperature. The absorbance was monitored at a wavelength of 505 nm.

The incorporation ratio (IR) of Chol was calculated as follows:

$$IR\ \% = \frac{\text{Incorporated mass of Chol}}{\text{Initial added mass of Chol}} \times 100 \quad \text{Eq. (2)}$$

Where the incorporated mass of Chol stands for the Chol mass determined in the liposome structure, the initial mass of Chol represents the mass initially used to prepare liposomes.

2.4.6 Encapsulation efficiency and loading ratio of Cyst

The EE and LR% of Cyst in liposomes were determined using the optimized Ellman method. 250 µL of the Cyst standard solution, the filtrate containing free Cyst, or the diluted solution of the liposomal suspension were added to 1.25 mL phosphate buffer, 1.25 mL of methanol, and 50 µL of Ellman's reagent. This method allows the determination of the free ($[Cyst]_{free}$) and the total ($[Cyst]_{tot}$) Cyst concentrations. EE% was calculated as the following equation:

$$EE_{cyst}\% = \frac{[Cyst]_{tot} - [Cyst]_{free}}{[Cyst]_{tot}} \times 100 \quad \text{Eq. (3)}$$

where $[Cyst]_{tot}$ and $[Cyst]_{free}$ correspond to the concentration of total and free Cyst in the liposomal suspension, respectively.

LR% of Cyst was calculated as follows:

$$LR\% = \frac{m_{total} - m_{free}}{m_{initial}} \times 100 \quad \text{Eq. (4)}$$

where m_{total} and m_{free} are the mass of total and free Cyst in the liposomal suspension and $m_{initial}$ is the mass of Cyst initially added to the aqueous phase during the preparation of the liposomes.

2.5 Stability study

The formulation PH 90H: Chol: Cyst (1:0.98:10) was selected to compare the stability of Cyst loaded in liposome to that of free Cyst. The liposomal suspension (5 mL) was centrifuged, the supernatant was eliminated, and the pellet was re-suspended in water. The concentration of the encapsulated Cyst was determined after the destruction of liposomes by sonication; Cyst solutions with a similar concentration were prepared in water and placed at 4, 25, and 37°C in the dark. Also, the same concentration of free Cyst was placed in light at 25°C. At different times, aliquots were removed, and the concentration of Cyst remaining in solution and that of formed cystamine were determined by ion-pair chromatography.

The percentage of remaining Cyst was calculated as follows:

$$\text{Remaining Cyst (\%)} = \frac{[\text{Cyst}]_t}{[\text{Cyst}]_{t0}} \times 100 \quad \text{Eq. (5)}$$

where $[\text{Cyst}]_t$ is the concentration of remaining Cyst determined at time t and $[\text{Cyst}]_{t0}$ is the initial Cyst concentration.

The percentage of formed cystamine was calculated as follows:

$$\text{Formed cystamine (\%)} = \frac{[\text{Cystamine}]_t}{[\text{Cystamine}]_f} \times 100 \quad \text{Eq. (6)}$$

where $[\text{Cystamine}]_t$ is the concentration of formed cystamine determined at time t and $[\text{Cystamine}]_f$ is the final cystamine concentration obtained after the total conversion of cysteamine to cystamine.

2.6 Freeze-drying of liposomes

The freeze-drying of blank and Cyst loaded liposomes composed of PH 90H and Chol was performed according to *Gharib et al.* (Gharib et al., 2018). Blank liposomes and Cyst loaded

liposomes (PH 90H: Chol: Cyst molar ratios of 1:0.98:1 and 1:0.98:10) were freshly prepared; 5 mL were then ultracentrifuged at 170000 g for 1 h at 4°C. The supernatant was removed, and the pellet was reconstituted in an aqueous solution of 50 mM HP-β-CD (2 mL). The samples were kept at -20°C overnight then placed into the drying chamber of Cryonext 23020 freeze-dryer (Trappes, France), pre-cooled to -20°C, then lowered to -40°C with a slow cooling profile of 0.5°C/min. The product was stabilized for 30 min at -38°C before the vacuum was applied. Primary drying was executed at a pressure of 150 µbar for 3 h at -10°C, then the temperature of the drying chamber was progressively increased to 5°C for 6 h at 250 µbar, to reach finally 10°C at 350 µbar for 9 h. The temperature was adjusted at a product temperature higher than that of the sublimation temperature of the water. During primary drying, the ice crystals are sublimated, resulting in the porous cake of the freeze-concentrated matrix. A secondary drying step for 10 h at 20°C and 100 µbar pressure was applied. This step is crucial to decrease the residual water content of the amorphous matrix. Finally, the vials were removed from the freeze-dryer, closed with rubber caps, and stored at 4°C. The lyophilized liposomes were then reconstructed with ultra-pure water to its original volume (5 mL) before characterization and further analysis.

2.7 Storage stability of freeze-dried forms

After four months of storage at 4°C, freeze-dried liposomes were resuspended in 5 mL water; the particle size, PdI, and zeta potential values of the obtained suspensions were determined. The remaining Cyst concentrations were measured using ion-pair chromatography. The following equation was used to determine the percentage of remaining Cyst:

$$\text{Percentage of remaining Cyst} = \frac{[\text{Cyst}]_t}{[\text{Cyst}]_{t0}} \times 100 \quad \text{Eq. (7)}$$

where $[Cyst]_t$ and $[Cyst]_{t0}$ are the total concentrations of Cyst in the liposomal suspension before and after storage of dried liposomes at 4°C for 4 months. The experiment was carried out in triplicate.

247

3. Results and Discussion

3.1 Liposomes characterization

3.1.1 Size, polydispersity index, and zeta potential

The characterization of liposomes composed of saturated (PH 90H) and unsaturated (Lipoid S100) phospholipids and Chol was realized by DLS. The mean particle size, polydispersity index (PdI), and zeta potential values were determined (**Table 1**).

Two populations were observed in blank and Cyst-loaded liposomes. The first population was nanometric and represented more than 94% of the suspensions. The second population was of a micrometric size and represented a negligible percentage varying between 1 and 6%.

The size of blank PH 90H liposomes was 211 ± 8 nm, while that of blank Lipoid S100 liposomes was lower (151 ± 11 nm). Similar results were obtained by *Gharib et al.* (Gharib et al., 2017).

The PdI values were close to 0.2 for all the formulations, signifying that the liposomes had homogeneous size. The zeta potential indicates the vesicle's surface charge; this parameter reflected the liposome stability since it shows repulsive forces between particles (Domingues et al., 2008). All liposomal formulations had a negative charge due to the presence of the phosphate group at the surface of the vesicles (Ascenso et al., 2013). Liposomes incorporating Cyst presented zeta potential values lower than blank ones. A variation of the pH between the supernatants of blank liposomal formulation (pH 7) and Cyst loaded liposomes (pH 9.5) was noticed. Also, the positively charged amino group of Cyst can interact with the negative charges of phosphate groups of lipid membranes. The decrease of zeta potential values could be due to the negative sulfur group of cysteamine attached to the surface. Indeed, after the incubation of Cyst with the blank liposomes, the centrifugation of the mixture, and the reconstitution of the pellet with water, the vesicles presented lower zeta potential values than blank liposomes indicating that electrostatic interaction between Cyst and liposomes surface may occur.

Berleur et al. studied the interaction of Cyst with dipalmitoylphosphatidylcholine (DPPC) using differential scanning calorimetry, electron spin resonance, and turbidimetry. They demonstrated that Cyst interacts with the DPPC membranes in their polar head region. At a low concentration (10^{-4} M), Cyst behaved like a divalent cation (amine and SH groups), creating electrostatic bridges with the negatively charged phosphate groups of the polar heads of lipids leading to an increase in membrane stability. These bridges are disrupted when Cyst is present at high concentration (10^{-2} and 10^{-1} M) inducing a decrease in the lipid membrane rigidity; Cyst acted like a monovalent cation and displacement of the slightly charged SH extremity by the amine of Cyst is occurred (Berleur et al., 1985).

3.1.2 Incorporation ratios of phospholipid and Chol, encapsulation efficiency and loading ratio of Cyst

The quantification of phospholipids showed a high incorporation ratio of phospholipids in all the formulations since the IR values were above 94 ± 1.41% (**Table 2**). Our results are in accordance with those of *Sebaaly et al.* for blank PH 90 liposomes (Sebaaly et al., 2016). Cyst did not affect the incorporation ratio of phospholipids since it is a hydrophilic molecule, and therefore, it is expected to be encapsulated in the aqueous core of the liposomes. Concerning Chol incorporation, the IR of Chol was higher for Lipoid S100 blank liposome (95 ± 2.0%) than for PH 90H blank liposome (80 ± 0.0%). Similar results were reported by *Azzi et al.*, where the IR values of Chol were higher for Lipoid S100 (85.2 ± 2.4%) when compared to PH 90H liposomes (84.2 ± 3.8%) (Azzi et al., 2018). Regarding Chol incorporation into Cyst-loaded liposomes, the IR% values were slightly decreased for Cyst-loaded PH 90H liposomes compared to blank liposomes. While for Lipoid S100-liposomes, a noticeable decrease of the IR of Chol was observed at high Cyst to lipid molar ratios (phospholipid:Chol:Cyst of 1:1.17:5.89 and 1:1.17:11.78). The mechanism underlying this decrease is unclear.

On the other hand, EE and LR% of Cyst decreased while increasing the concentration of Cyst in both types of liposomes. The higher EE and LR% values were obtained for the liposomal

suspensions containing the lowest concentration of Cyst **(Table 2)**. At this same Cyst concentration, the EE and the LR% of Cyst were higher for unsaturated liposomes when compared to saturated ones. The preparation of PH 90H liposomes required heating above the main transition temperature of the phospholipid (55°C), which could accelerate the oxidation of the product. The EE% values of Cyst were generally lower (less than 40%) than those determined for hydrophobic bioactive molecules (Azzi et al., 2018; Sebaaly et al., 2015) using the same liposome formulations. A low encapsulation efficiency usually results when encapsulating a hydrophilic drug (Eloy et al., 2014) because of its diffusion in and out of the lipid membrane. Thus, the drug is difficultly retained inside the liposomes (Çağdaş et al., 2014). The EE% values of caffeine were 7, 18, and 30% in Lipoid S100, Phospholipon 90G (phosphatidylcholine 95%) liposomes (Tuncay Tanriverdi, 2018), and egg or soy lecithin (Budai, 2013). Also, the EE% value of ciprofloxacin was 9% in liposomes composed of 1,2-distearoyl-sn-glycero-3-phosphoglycerol-distearoylphosphatidylcholine-Chol (5:5:5 molar ratio) (Oh et al., 1995); that of mitomycin C was 31% in Phospholipon 80:Chol (9:6 molar ratio) (Chetoni et al., 2007) and the EE% value of ascorbic acid was 40% in phosphatidylcholine liposomes (Serrano et al., 2015).

3.1.3 Liposomes morphology

TEM images of blank liposomes and Cyst-loaded liposomes are shown in **Fig. 2**. These images correlated with the DLS results and showed the formation of nanometer-sized vesicles. Oligolamellar spherical-shaped vesicles were obtained for blank and Cyst-loaded liposomes.

3.2 Stability study

The stability of free and encapsulated Cyst was assessed at different temperatures (4, 25, and 37°C) and in dark and light. Aliquots were withdrawn at different time intervals, and the concentration of Cyst was determined by ion-pair chromatography. The results were

expressed as the percentage of Cyst remaining in the solution as a function of time. The plots showed a straight line indicating that the oxidation of Cyst followed a zero-order reaction, and the slope corresponds to –k.

The stability of Cyst decreased when the temperature increased **(Fig. 3)**. Cyst was oxidized after 15 h at 4°C in the dark with a degradation rate of 5.25 ± 0.09 $\mu g.mL^{-1}.h^{-1}$ (**Table 3**). Whereas at 37°C in the dark, the total oxidation of Cyst was achieved after 8h of incubation with a degradation rate of 11.52 ± 0.16 $\mu g.mL^{-1}.h^{-1}$. *Pescina et al.* confirmed the temperature dependence of Cyst oxidation after measuring the stability of the molecule at -20, 4, and 25°C (Pescina et al., 2016).

The effect of light on Cyst stability was also evaluated, and the results showed that there wasn't any significant difference between the stability of incubated Cyst in light or dark **(Fig. 4)**. The degradation rate of Cyst was slightly higher at 25°C in light (10.68 ± 0.57 $\mu g.mL^{-1}.h^{-1}$) than in dark (10.06 ± 0.07 $\mu g.mL^{-1}.h^{-1}$).

The encapsulation of Cyst slowed down the oxidation of Cyst in all the studied conditions. For example, at 4°C in the dark, the total oxidation was delayed for 43 h for the encapsulated Cyst compared to the free Cyst. The protection factor, defined as the degradation rate of the free Cyst divided by the degradation rate of the encapsulated Cyst, was also calculated. Following the encapsulation of Cyst in liposomes, protection factors from its oxidation were of 2.96, 4.7, 5, and 4.14 after storage at 4°C, 25°C at dark, 25°C in light, and 37°C, respectively (**Table 3**). Whereas, the use of cyclodextrin didn't affect the stability of Cyst (Pescina et al., 2016). Besides, *Dixon et al.* found that the addition of antioxidants except the enzyme catalase had an insignificant effect on the prevention of Cyst oxidation (Dixon et al., 2018).

To our knowledge, the quantification of Cyst and its degradation product cystamine is done for the first time in liposomal suspension. Cyst was totally converted to cystamine. The latter

was the only product present in the liposomal suspension after the total oxidation of Cyst. The encapsulation delayed this conversion in all the studied conditions **(Fig. 5)**.

3.3 Freeze-drying

Gharib et al. succeeded to freeze-dry PH 90H liposomes formulations using HP-β-CD (50 mM) as a cryoprotectant (Gharib et al., 2018). Two formulations of Cyst loaded liposomes (PH 90H:Chol:Cyst 1:0.98:1 and 1:0.98:10 molar ratios) were selected for freeze-drying. The liposomes were then reconstituted in water and characterized for their morphology, homogeneity, size, surface charge, and LR% (**Table 4**).

The morphology of the liposomes was preserved after lyophilization (**Fig. 6**); the vesicles appeared to be oligolamellar and spherical. The presence of HP-β-CD did not affect liposome lamellarity or morphology.

The size of blank and Cyst PH 90H loaded liposomes was maintained after lyophilization regardless of the concentration of Cyst. A slight increase of the pdI values was observed after lyophilization and reconstitution for blank and Cyst-loaded liposomes. The zeta potential value was conserved for the blank liposomes; nevertheless, it significantly decreased for Cyst-loaded liposomes from -42 to -19 mV for the formulation PH 90H:Chol:Cyst molar ratio of 1:0.98:1 and from -48 to -33 mV for the formulation PH 90H:Chol:Cyst molar ratio of 1:0.98:10. The variation of the zeta potential was due to the loss of Cyst bound to the outer side of the membranes of the vesicles during lyophilization. Furthermore, the loading ratio of Cyst after the freeze-drying decreased from 24 to 8% in PH 90H:Chol:Cyst (1:0.98:1) and from 16 to 5% in PH 90H:Chol:Cyst (1:0.98:10). After lyophilization, liposomal suspension retained 33% of Cyst present in the PH 90H liposomal suspension. A significant decrease in the loading rate of anethole after freeze-drying in anethole loaded liposomes was also observed previously (Gharib et al., 2018).

3.4 Storage stability of freeze-dried forms

The mean particle size, PdI, and zeta potential values of the reconstituted liposomes after freeze-drying and after four months of storage at 4°C were evaluated (**Table 4**). The two formulations used in this study were stable with adequate size, PdI, and zeta potential values. Besides, the total concentrations of Cyst in the reconstituted liposomes after freeze-drying were determined after four months and compared to those obtained at t_0. The percentage of remaining Cyst was 16% for the formulation PH 90H:Chol:Cyst (1:0.98:10). This result was satisfactory, especially when considering the high instability of Cyst; Cyst was oxidized entirely to Cystamine after 15 h in aqueous solution and 60 h in liposomal suspensions after storage at 4°C (**Fig. 3A**). The storage conditions are critical in the case of Cyst. Taking into account its instability, the eye-drop Cystaran™ (Cyst ophthalmic solution 0.44%) has to be stored at -20°C, and administered hourly during the daytime. After its opening, it should be used within one week (Huynh et al., 2013). Cyst hydrochloride (0.5%) formulated ophthalmic preparation is easily oxidized within the first week after storage at +4°C, rendering the preparation less effective (Reda et al., 2017). In comparison with the aqueous liposomal suspension, the freeze-dried form conserved Cyst for a more extended period. The elimination of the water from the liposomal suspension is the factor that induced this improvement of Cyst stability. The presence of water will lead to the degradation of Cyst to cystamine (Gana et al., 2015).

4. Conclusion

In this study, we proved that the encapsulation of Cyst in conventional liposomes improved its stability. Cyst-loaded liposomes were nanometric and presented a negative surface charge. In addition to its incorporation in vesicles, Cyst binds to the surface of the vesicle. The loading ratio of Cyst in liposomes varied between 12 and 24% depending on Cyst to lipid molar ratio. Besides, in this work, we succeeded in preparing freeze-dried liposomes that retain a noticeable amount of Cyst after four months of storage at 4°C. These results could help to develop various pharmaceutical forms of Cyst and enlarge its applications.

Acknowledgements

Authors thank the Research Funding Program at the Lebanese University and the "Agence Universitaire de la Francophonie, projet PCSI" for supporting the project (2018-2020). Authors also thank Géraldine Agusti for the TEM measurements. Electron microscopy studies have been done at the "Centre Technologique des Microstructures" – Claude Bernard University of Lyon.

Declaration of Competing Interest

The authors declare that they have no known competing financial interests or personal relationships that could have appeared to influence the work reported in this paper.

References

Apffel, C.A., Walker, J.E., Issarescu, S., 1975. Tumor Rejection in Experimental Animals Treated with Radioprotective Thiols. Cancer Res 35, 429–437.

Ascenso, A., Cruz, M., Euletério, C., Carvalho, F.A., Santos, N.C., Marques, H.C., Simões, S., 2013. Novel tretinoin formulations: a drug-in-cyclodextrin-in-liposome approach. Journal of Liposome Research 23, 211–219. https://doi.org/10.3109/08982104.2013.788026

Atallah, C., Charcosset, C., Greige-Gerges, H., 2020. Challenges for cysteamine stabilization, quantification, and biological effects improvement. Journal of Pharmaceutical Analysis. https://doi.org/10.1016/j.jpha.2020.03.007

Azzi, J., Auezova, L., Danjou, P.-E., Fourmentin, S., Greige-Gerges, H., 2018. First evaluation of drug-in-cyclodextrin-in-liposomes as an encapsulating system for nerolidol. Food Chemistry 255, 399–404. https://doi.org/10.1016/j.foodchem.2018.02.055

Bacq, Z.M., Dechamps, G., Fischer, P., Herve, A., Le Bihan, H., Lecomte, J., Pirotte, M., Rayet, P., 1953. Protection against x-rays and therapy of radiation sickness with beta-mercaptoethylamine. Science 117, 633–636.

Berleur, F., Roman, V., Jaskierowicz, D., Fatome, M., Leterrier, F., Ter-Minassian-Saraga, L., Madelmont, G., 1985. The binding of the radioprotective agent cysteamine with the phospholipidic membrane headgroup-interface region. Biochem. Pharmacol. 34, 3071–3080.

Besouw, M., Masereeuw, R., van den Heuvel, L., Levtchenko, E., 2013. Cysteamine: an old drug with new potential. Drug Discovery Today 18, 785–792. https://doi.org/10.1016/j.drudis.2013.02.003

Bozdağ, S., Gümüş, K., Gümüş, O., Unlü, N., 2008. Formulation and in vitro evaluation of cysteamine hydrochloride viscous solutions for the treatment of corneal cystinosis. Eur J Pharm Biopharm 70, 260–269. https://doi.org/10.1016/j.ejpb.2008.04.010

Budai, L., 2013. Liposomes for Topical Use: A Physico-Chemical Comparison of Vesicles Prepared from Egg or Soy Lecithin. Scientia Pharmaceutica 81, 1151–1166. https://doi.org/10.3797/scipharm.1305-11

Butler, J.D., Tietze, F., Pellefigue, F., Spielberg, S.P., Schulman, J.D., 1978. Depletion of Cystine in Cystinotic Fibroblasts by Drugs Enclosed in Liposomes. Pediatric Research 12, 46–51. https://doi.org/10.1203/00006450-197801000-00012

Çağdaş, M., Sezer, A.D., Bucak, S., 2014. Liposomes as Potential Drug Carrier Systems for Drug Delivery. Application of Nanotechnology in Drug Delivery. https://doi.org/10.5772/58459

Chavin, W., Schlesinger, W., 1966. Some potent melanin depigmentary agents in the black goldfish. Naturwissenschaften 53, 413–414.

Chetoni, P., Burgalassi, S., Monti, D., Najarro, M., Boldrini, E., 2007. Liposome-encapsulated mitomycin C for the reduction of corneal healing rate and ocular toxicity. Journal of Drug Delivery Science and Technology 17, 43–48. https://doi.org/10.1016/S1773-2247(07)50006-7

Dixon, P., Powell, K., Chauhan, A., 2018. Novel approaches for improving stability of cysteamine formulations. International Journal of Pharmaceutics 549, 466–475. https://doi.org/10.1016/j.ijpharm.2018.08.006

Domingues, M.M., Santiago, P.S., Castanho, M.A.R.B., Santos, N.C., 2008. What can light scattering spectroscopy do for membrane-active peptide studies? Journal of Peptide Science 14, 394–400. https://doi.org/10.1002/psc.1007

Elmonem, M.A., Veys, K.R., Soliman, N.A., van Dyck, M., van den Heuvel, L.P., Levtchenko, E., 2016. Cystinosis: a review. Orphanet Journal of Rare Diseases 11, 47. https://doi.org/10.1186/s13023-016-0426-y

Eloy, J.O., Claro de Souza, M., Petrilli, R., Barcellos, J.P.A., Lee, R.J., Marchetti, J.M., 2014. Liposomes as carriers of hydrophilic small molecule drugs: Strategies to enhance encapsulation and delivery. Colloids and Surfaces B: Biointerfaces 123, 345–363. https://doi.org/10.1016/j.colsurfb.2014.09.029

Farshi, S., Mansouri, P., Kasraee, B., 2018. Efficacy of cysteamine cream in the treatment of epidermal melasma, evaluating by Dermacatch as a new measurement method: a randomized double blind placebo controlled study. Journal of Dermatological Treatment 29, 182–189. https://doi.org/10.1080/09546634.2017.1351608

Frenk, E., Pathak, M.A., Szabó, G., Fitzpatrick, T.B., 1968. Selective action of mercaptoethylamines on melanocytes in mammalian skin: experimental depigmentation. Arch Dermatol 97, 465–477.

Gallego-Villar, L., Hannibal, L., Häberle, J., Thöny, B., Ben-Omran, T., Nasrallah, G.K., Dewik, A.-N., Kruger, W.D., Blom, H.J., 2017. Cysteamine revisited: repair of arginine to cysteine mutations. Journal of Inherited Metabolic Disease 40, 555–567. https://doi.org/10.1007/s10545-017-0060-4

Gana, I., Barrio, M., Ghaddar, C., Nicolaï, B., Do, B., Tamarit, J.-L., Safta, F., Rietveld, I.B., 2015. An Integrated View of the Influence of Temperature, Pressure, and Humidity on the Stability of Trimorphic Cysteamine Hydrochloride. Molecular Pharmaceutics 12, 2276–2288. https://doi.org/10.1021/mp500830n

Gharib, R., Auezova, L., Charcosset, C., Greige-Gerges, H., 2017. Drug-in-cyclodextrin-in-liposomes as a carrier system for volatile essential oil components: Application to anethole. Food Chem 218, 365–371. https://doi.org/10.1016/j.foodchem.2016.09.110

Gharib, R., Greige-Gerges, H., Fourmentin, S., Charcosset, C., 2018. Hydroxypropyl-ß-cyclodextrin as a membrane protectant during freeze-drying of hydrogenated and non-hydrogenated liposomes and molecule-in-cyclodextrin-in- liposomes: Application to trans-anethole. Food Chemistry 267, 67–74. https://doi.org/10.1016/j.foodchem.2017.10.144

Gresham, P.A., Barnett, M., Smith, S.V., Schneider, R., 1971. Use of a sustained-release multiple emulsion to extend the period of radio protection conferred by cysteamine. Nature 234, 149–150.

Huynh, N., Gahl, W.A., Bishop, R.J., 2013. Cysteamine ophthalmic solution 0.44% for the treatment of corneal cystine crystals in cystinosis. Expert Review of Ophthalmology 8, 341–345. https://doi.org/10.1586/17469899.2013.814885

Ijaz, M., Ahmad, M., Akhtar, N., Laffleur, F., Bernkop-Schnürch, A., 2016. Thiolated α-Cyclodextrin: The Invisible Choice to Prolong Ocular Drug Residence Time. Journal of Pharmaceutical Sciences 105, 2848–2854. https://doi.org/10.1016/j.xphs.2016.04.021

Ijaz, M., Matuszczak, B., Rahmat, D., Mahmood, A., Bonengel, S., Hussain, S., Huck, C.W., Bernkop-Schnürch, A., 2015. Synthesis and characterization of thiolated β-cyclodextrin as a novel mucoadhesive excipient for intra-oral drug delivery. Carbohydrate Polymers 132, 187–195. https://doi.org/10.1016/j.carbpol.2015.06.073

Jaskierowicz, D., Genissel, F., Roman, V., Berleur, F., Fatome, M., 1985. Oral Administration of Liposome-entrapped Cysteamine and the Distribution Pattern in Blood, Liver and Spleen. International Journal of Radiation Biology and Related Studies in Physics, Chemistry and Medicine 47, 615–619. https://doi.org/10.1080/09553008514550851

Jeitner, T.M., Oliver, J.R., 1990. Possible oncostatic action of cysteamine on the pituitary glands of oestrogen-primed hyperprolactinaemic rats. Journal of Endocrinology 127, 119–127. https://doi.org/10.1677/joe.0.1270119

Lahiani-Skiba, M., Boulet, Y., Youm, I., Bounoure, F., Vérité, P., Arnaud, P., Skiba, M., 2007. Interaction between hydrophilic drug and α-cyclodextrins: physico-chemical aspects. Journal of Inclusion Phenomena and Macrocyclic Chemistry 57, 211–217. https://doi.org/10.1007/s10847-006-9194-y

Laouini, A., Jaafar-Maalej, C., Limayem-Blouza, I., Sfar, S., Charcosset, C., Fessi, H., 2012. Preparation, Characterization and Applications of Liposomes: State of the Art. Journal of Colloid Science and Biotechnology 1, 147–168. https://doi.org/10.1166/jcsb.2012.1020

Mansouri, P., Farshi, S., Hashemi, Z., Kasraee, B., 2015. Evaluation of the efficacy of cysteamine 5% cream in the treatment of epidermal melasma: a randomized double-blind placebo-controlled trial. Br. J. Dermatol. 173, 209–217. https://doi.org/10.1111/bjd.13424

Min-Oo, G., Fortin, A., Poulin, J.-F., Gros, P., 2010. Cysteamine, the Molecule Used To Treat Cystinosis, Potentiates the Antimalarial Efficacy of Artemisinin. Antimicrobial Agents and Chemotherapy 54, 3262–3270. https://doi.org/10.1128/AAC.01719-09

Oh, Y.K., Nix, D.E., Straubinger, R.M., 1995. Formulation and efficacy of liposome-encapsulated antibiotics for therapy of intracellular Mycobacterium avium infection. Antimicrob. Agents Chemother. 39, 2104–2111. https://doi.org/10.1128/aac.39.9.2104

Pescina, S., Carra, F., Padula, C., Santi, P., Nicoli, S., 2016. Effect of pH and penetration enhancers on cysteamine stability and trans-corneal transport. European Journal of Pharmaceutics and Biopharmaceutics 107, 171–179. https://doi.org/10.1016/j.ejpb.2016.07.009

Reda, A., Van Schepdael, A., Adams, E., Paul, P., Devolder, D., Elmonem, M.A., Veys, K., Casteels, I., van den Heuvel, L., Levtchenko, E., 2017. Effect of Storage Conditions on Stability of Ophthalmological Compounded Cysteamine Eye Drops. JIMD Rep 42, 47–51. https://doi.org/10.1007/8904_2017_77

Sagar, S.M., Millard, W.J., Martin, J.B., Murchison, S.C., 1985. The mechanism of action of cysteamine in depleting prolactin immunoreactivity. Endocrinology 117, 591–600. https://doi.org/10.1210/endo-117-2-591

Sebaaly, C., Greige-Gerges, H., Stainmesse, S., Fessi, H., Charcosset, C., 2016. Effect of composition, hydrogenation of phospholipids and lyophilization on the characteristics of eugenol-loaded liposomes prepared by ethanol injection method. Food Bioscience 15, 1–10. https://doi.org/10.1016/j.fbio.2016.04.005

Sebaaly, C., Jraij, A., Fessi, H., Charcosset, C., Greige-Gerges, H., 2015. Preparation and characterization of clove essential oil-loaded liposomes. Food chemistry 178, 52–62. https://doi.org/10.1016/j.foodchem.2015.01.067

Serrano, G., Almudéver, P., Serrano, J.-M., Milara, J., Torrens, A., Expósito, I., Cortijo, J., 2015. Phosphatidylcholine liposomes as carriers to improve topical ascorbic acid treatment of skin disorders. Clin Cosmet Investig Dermatol 8, 591–599. https://doi.org/10.2147/CCID.S90781

Tuncay Tanriverdi, S., 2018. Preparation and Characterization of Caffeine Loaded Liposome and Ethosome Formulations for Transungual Application. The Turkish Journal of Pharmaceutical Sciences 15, 178–183. https://doi.org/10.4274/tjps.22931

Zylberberg, C., Matosevic, S., 2016. Pharmaceutical liposomal drug delivery: a review of new delivery systems and a look at the regulatory landscape. Drug Deliv 23, 3319–3329. https://doi.org/10.1080/10717544.2016.1177136

Figures Legends

Figure 1: Structure of Cyst.

Figure 2: TEM images for blank PH 90H liposomes (A), Cyst-loaded PH 90H liposomes (PH 90H: Chol: Cyst 1:0.98:1) (B) blank Lipoid S100 liposomes (C), Cyst-loaded Lipoid S100 liposomes (Lipoid S100: Chol: Cyst 1: 1.17: 1.77) (D).

Figure 3: Stability study of free and encapsulated Cyst in the dark at 4°C (A), 25°C (B), and 37°C (C).

Figure 4: Stability study of free and encapsulated Cyst at 25°C in the dark (A) and in light (B).

Figure 5: Percentage of formed cystamine in free and Cyst-loaded liposomes in the dark at 4°C (A), 25°C (dark (B), and light (C)), and 37°C (D).

Figure 6: TEM images for blank (A) and Cyst-loaded-PH 90H liposomes (B) after freeze-drying and reconstitution with water.

574

Figure(s)

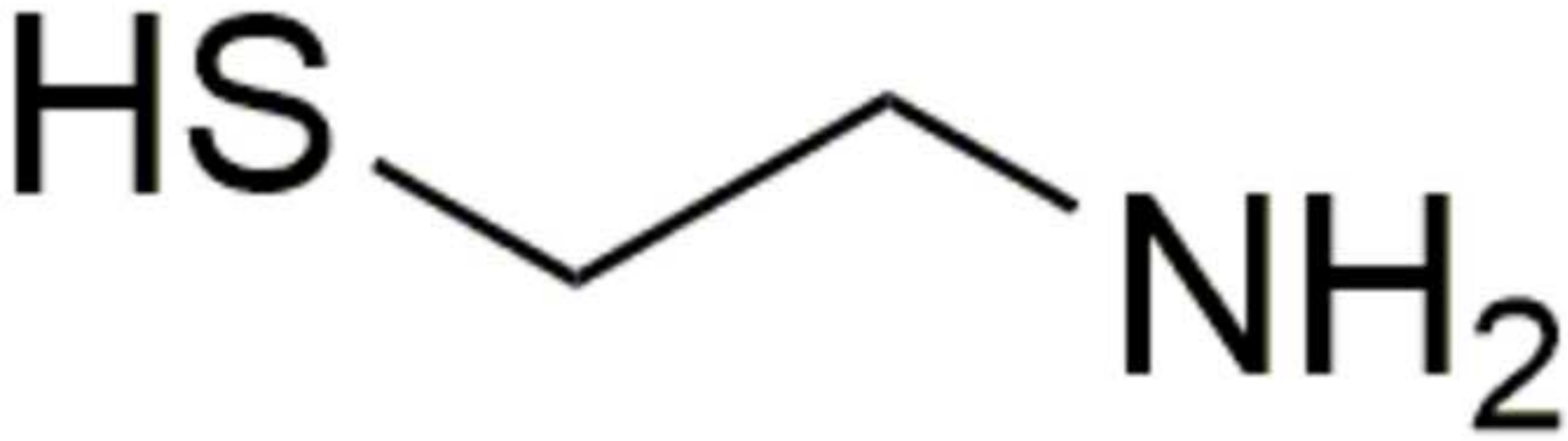

Figure 2

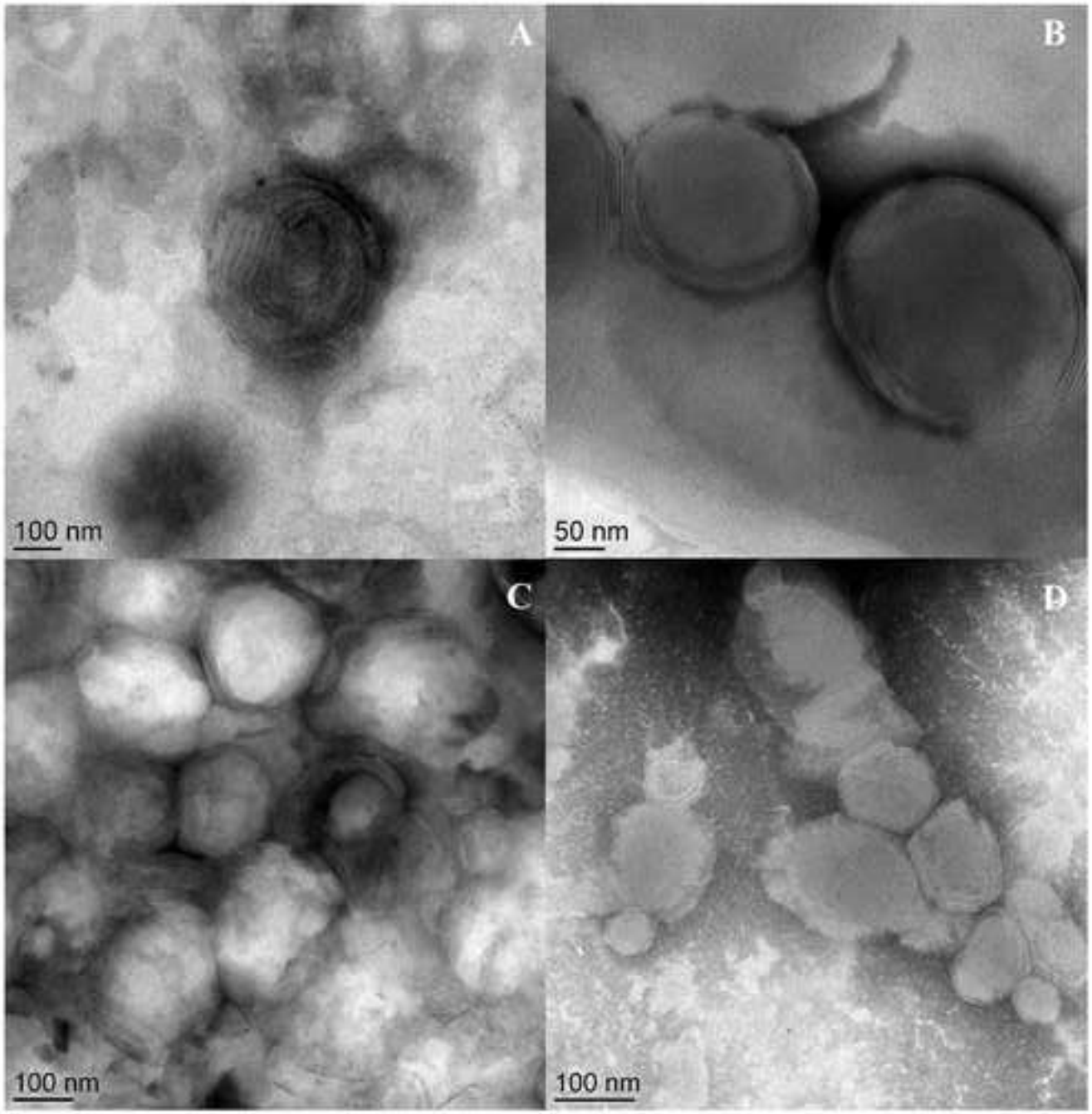

Figure 3

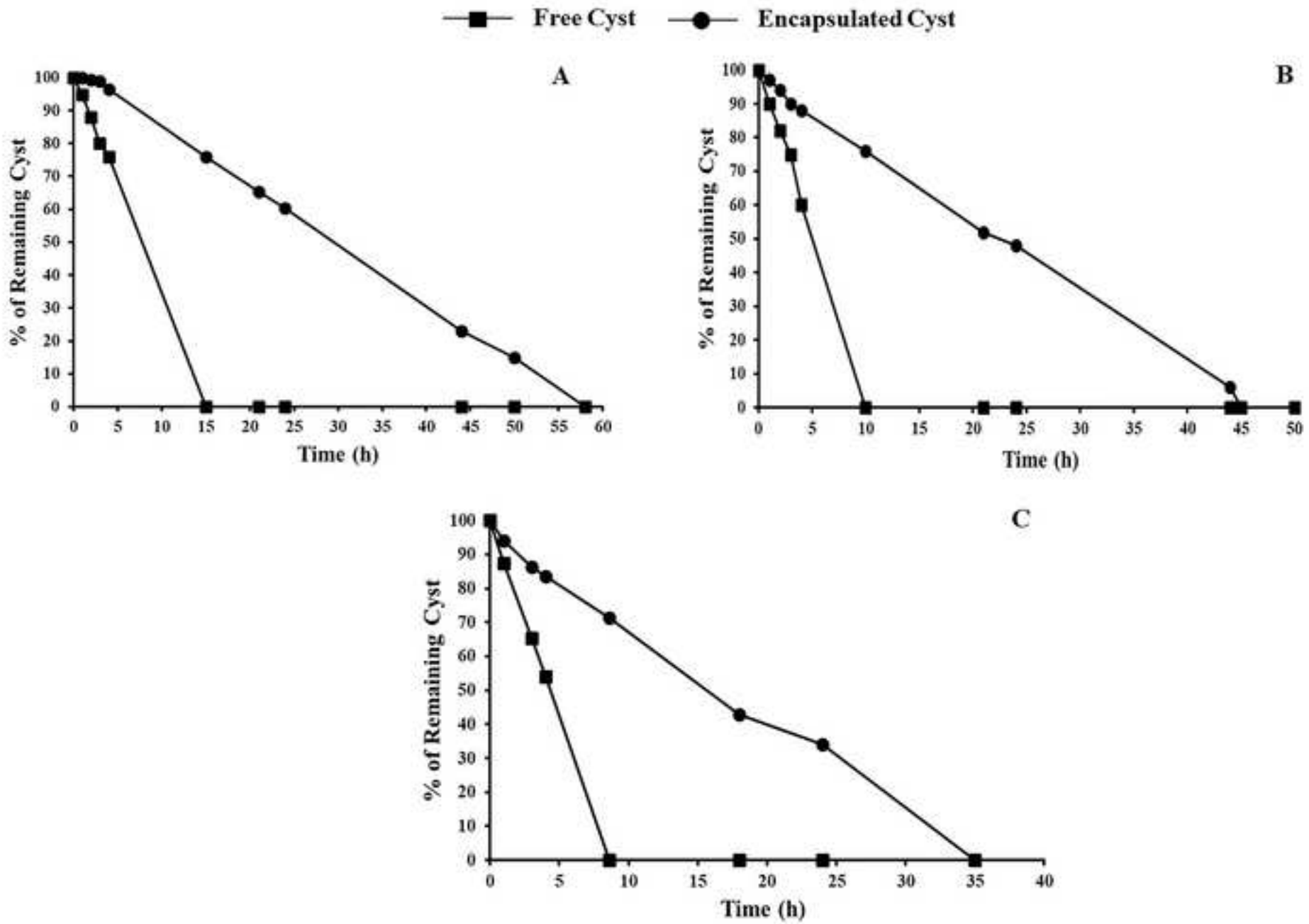

Figure 4

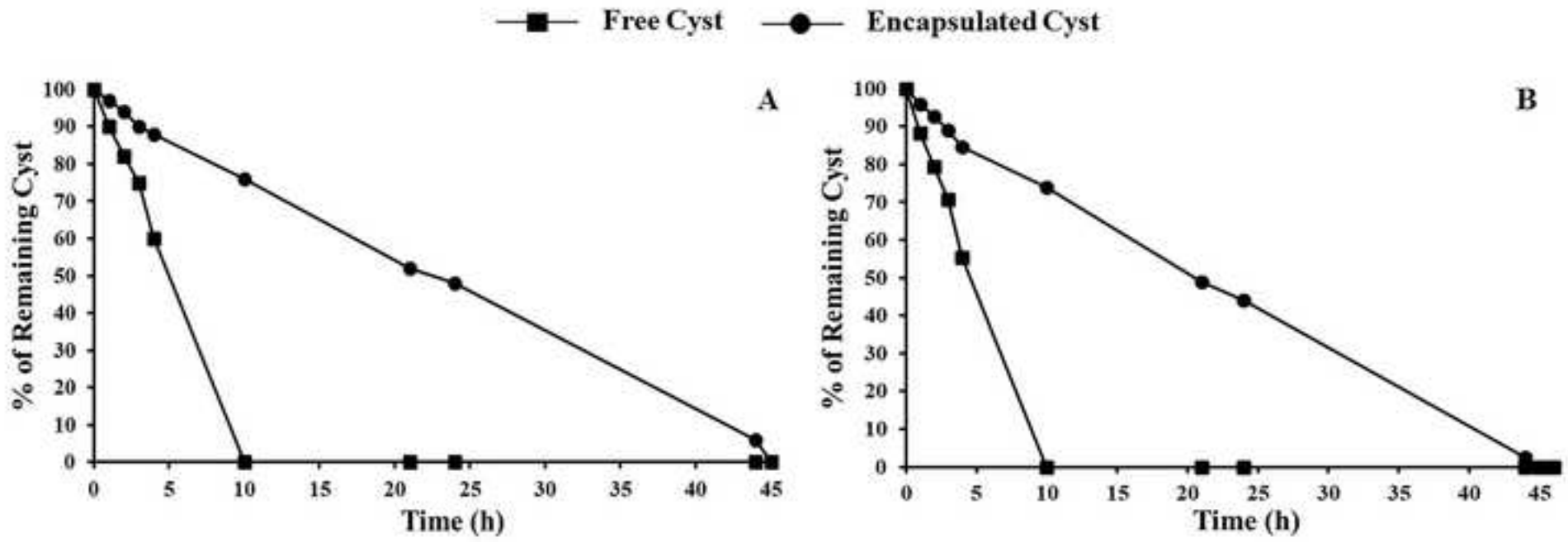
Free Cyst
Encapsulated Cyst
A
B
% of Remaining Cyst
Time (h)
0
10
20
30
40
50
60
70
80
90
100
0
5
10
15
20
25
30
35
40
45

Figure 5

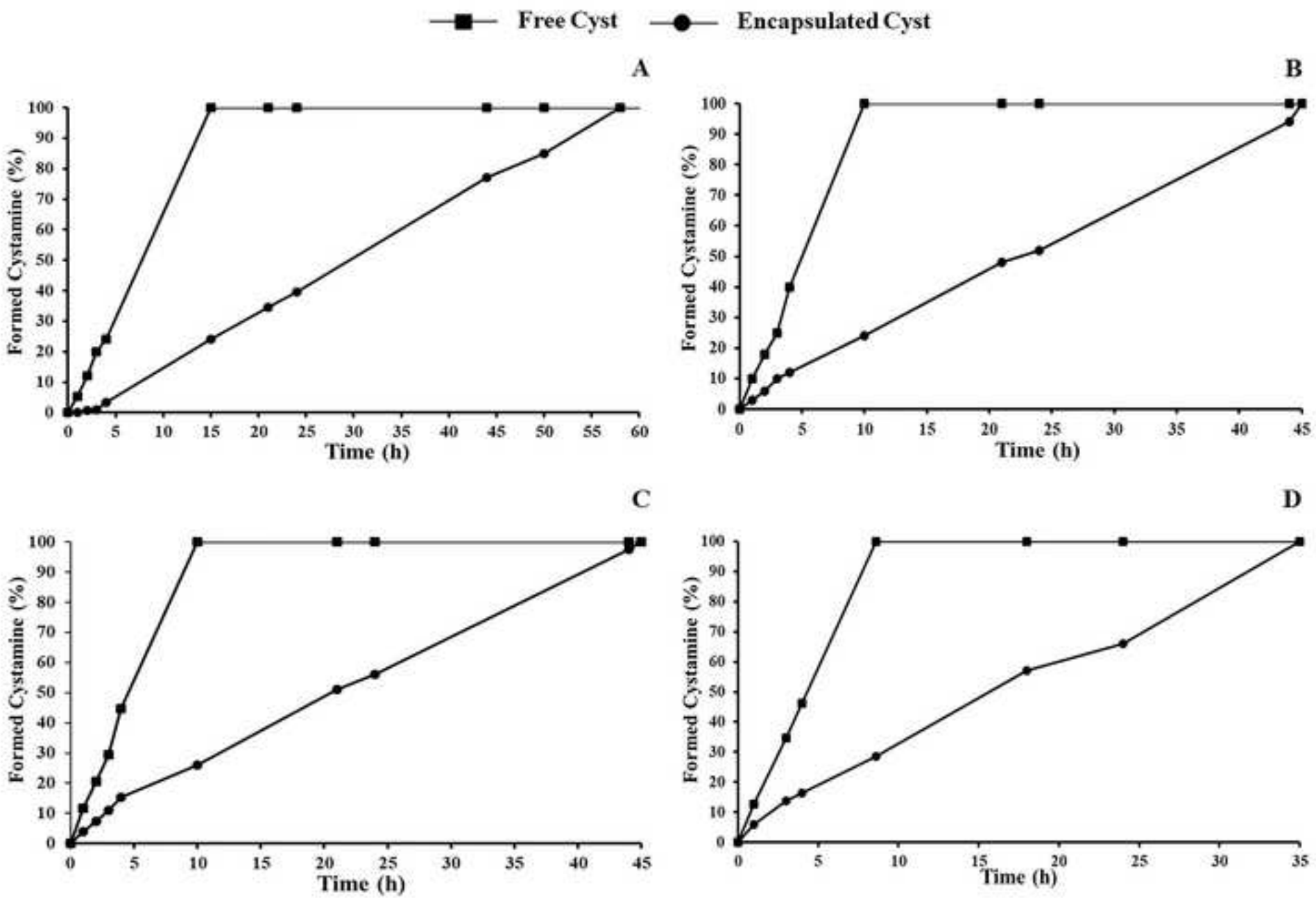

Figure 6

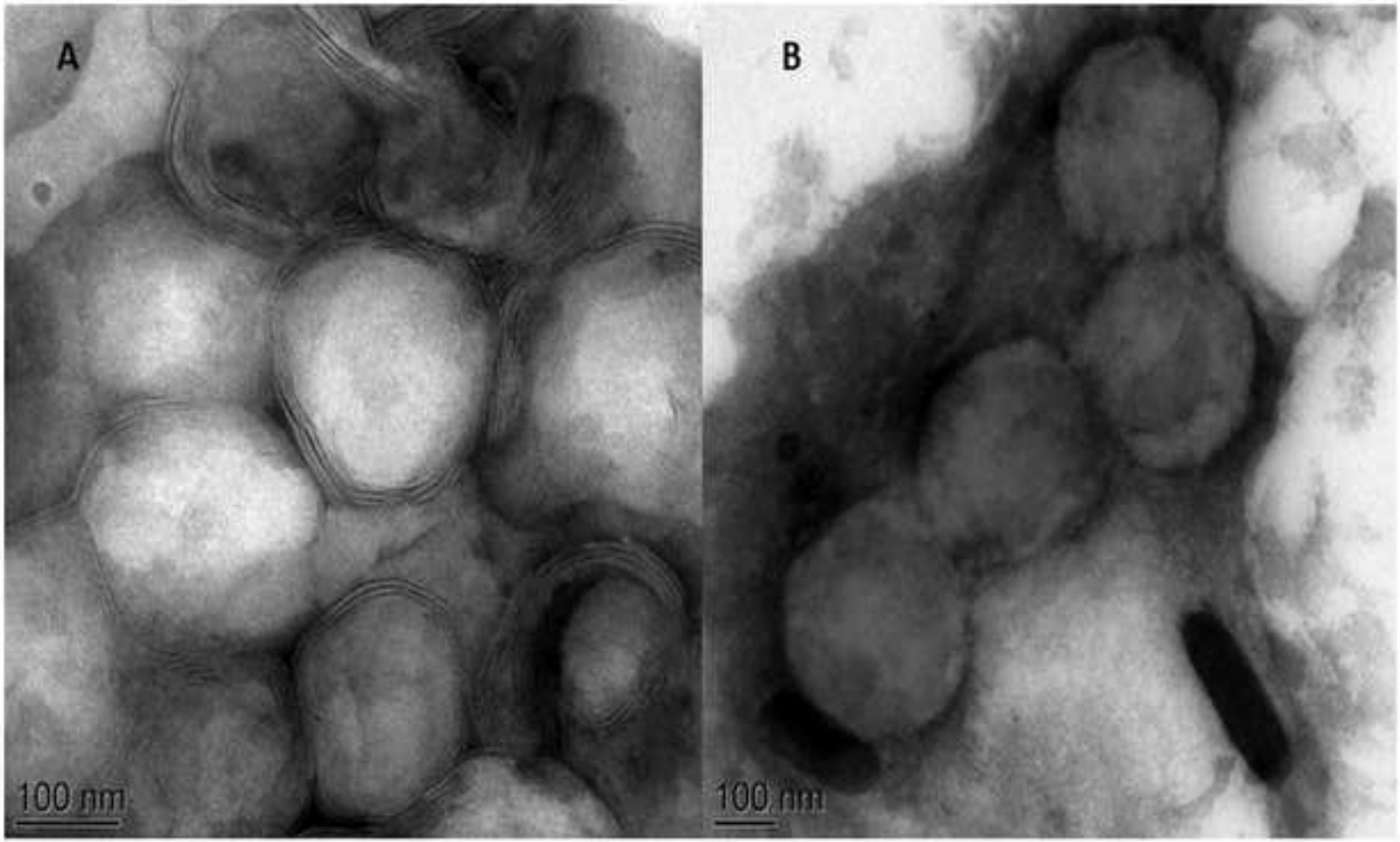

Table(s)

Table 1: Size, pdI, and zeta potential of blank and Cyst loaded PH 90H and Lipoid S100 liposomes.

Formulation	Lipid:Chol: Cyst molar ratio	Size				Zeta potential (mV)	PdI
		Population 1		Population 2			
		%	Mean size (nm)	%	Mean size (µm)		
Blank liposomes (PH 90H:Chol)	1:0.98	99 ± 0.4	211 ± 8	0.9 ± 0.4	5 ± 0.1	-17.9 ± 4.0	0.2 ± 0.0
Cyst-loaded liposomes (PH 90H:Chol:Cyst)	1:0.98:1	98 ± 1.3	301 ± 56	2 ± 1.3	5 ± 0.3	-35.8 ± 0.8	0.2 ± 0.0
	1:0.98:1.5	98 ± 1.1	318 ± 47	2 ± 1.1	5 ± 0.3	-37.1 ± 0.7	0.2 ± 0.1
	1:0.98:2	98 ± 1.7	248 ± 86	2 ± 1.7	5 ± 3.0	-37.0 ± 1.2	0.2 ± 0.1
	1:0.98:5	97 ± 2.7	278 ± 55	3 ± 2.7	5 ± 2.9	-45.0 ± 2.8	0.2 ± 0.1
	1:0.98:10	95 ± 0.7	262 ± 33	5 ± 0.7	5 ± 0.1	-45.0 ± 1.0	0.2 ± 0.1
Blank liposomes (Lipoid S100:Chol)	1:1.17	98 ± 0.7	151 ± 11	2 ± 0.0	5 ± 0.0	-24.0 ± 0.1	0.2 ± 0.0
Cyst loaded liposomes (Lipoid S100:Chol:Cyst)	1:1.17:1.17	94 ± 2.0	156 ± 13	6 ± 2.0	5 ± 0.2	-32.0 ± 0.41	0.3 ± 0.0
	1:1.17:1.77	97 ± 1.0	150 ± 3	3 ± 1.0	5 ± 0.3	-34.0 ± 3.70	0.3 ± 0.0
	1:1.17:2.36	97 ± 1.0	149 ± 1	3 ± 1.0	5 ± 1.0	-34.3 ± 1.45	0.3 ± 0.0
	1:1.17:5.89	97 ± 1.0	152 ± 11	3 ± 1.0	5 ± 0.2	-42.5 ± 1.17	0.3 ± 0.1
	1:1.17:11.78	97 ± 1.6	160 ± 8	3 ± 1.8	4 ± 0.2	-39.2 ± 1.30	0.2 ± 0.0

Table 2: Incorporation ratios of phospholipids (%) and Chol (%), EE%, and LR% values of Cyst in liposomes suspensions.

Formulations	Lipid:Chol:Cyst molar ratios	IR % of phospholipid	IR % of Chol	EE%	LR%	Final liposome composition (Lipid:Chol:Cyst molar ratio)
Blank liposomes (PH 90H:Chol)	1:0.98	94 ± 1.4	80 ± 0.0			0.94:0.81
Cyst-loaded liposomes (PH 90H:Chol:Cyst)	1:0.98:1	97 ± 0.8	74 ± 0.5	29 ± 3.0	24 ± 2	0.97:0.72:0.24
	1:0.98:1.5	100 ± 0.0	74 ± 1.5	26 ± 6.0	22 ± 6	1:0.72:0.33
	1:0.98:2	98 ± 0.5	72 ± 3.7	23 ± 4.0	20 ± 4	0.98:0.70:0.40
	1:0.98:5	94 ± 3.6	72 ± 2.0	24 ± 2.0	18 ± 3	0.94:0.70:0.90
	1:0.98:10	94 ± 2.5	74 ± 2.5	21 ± 5.0	16 ± 4	0.94:0.73:0.16
Blank liposomes (Lipoid S100:Chol)	1:1.17	99 ± 1.0	95 ± 2.0			0.99:1.11
Cyst loaded liposomes (Lipoid S100:Chol:Cyst)	1:1.17:1.17	100 ± 1.0	99 ± 2.0	40 ± 4.0	30 ± 2	0.99:1.16:0.35
	1:1.17:1.77	100 ± 2.0	91 ± 3.8	29 ± 4.0	24 ± 4	1:1.06:0.42
	1:1.17:2.36	99 ± 0.7	97 ± 5.0	22 ± 0.4	20 ± 1	0.99:1.13:0.47
	1:1.17:5.89	99 ± 1.0	35 ± 2.7	13 ± 2.0	12 ± 2	0.94:0.34:0.71
	1:1.17:11.78	99 ± 1.3	12 ± 0.0	13 ± 2.0	12 ± 2	0.94:0.12:1.41

Table 3: Degradation rate constants of free and encapsulated Cyst at 4°C (dark), 25°C (dark and light), and 37°C (dark).

Formulations	Temperature (°C)	Degradation rate constant k ($\mu g.\ mL^{-1}.h^{-1}$)	Protection factor
Free Cyst	4 (dark)	5.25 ± 0.09	-
Cyst loaded liposome		1.77 ± 0.18	2.96
Free Cyst	25 (dark)	10.06 ± 0.07	-
Cyst loaded liposome		2.14 ± 0.12	4.7
Free Cyst	25 (light)	10.68 ± 0.57	-
Cyst loaded liposome		2.12 ± 0.07	5
Free Cyst	37 (dark)	11.52 ± 0.16	-
Cyst loaded liposome		2.78 ± 0.05	4.14

Table 4: Size, polydispersity index, zeta potential values for blank and Cyst-loaded liposomes and loading rate of Cyst in liposomes made from PH 90H before and after freeze-drying at t_0 and after four months of storage in powder form **(bold)**. The values obtained after lyophilization were compared to those before lyophilization.

	Before freeze-drying				**After freeze-drying**			
	Size (nm)	**pdI**	**Zeta potential (mV)**	**LR%**	**Size (nm)**	**pdI**	**Zeta potential (mV)**	**LR%**
Blank PH 90H liposome	187 ± 42	0.15 ± 0.08	-17 ± 2.8		172 ± 14	0.23 ± 0.03	-18 ± 2.5	
PH 90H:Chol:Cyst 1:0.98:1	181 ± 19	0.12 ± 0.01	-37 ± 0.2	24 ± 2	166 ± 2 **231 ± 36**	0.15 ± 0.05 **0.29 ± 0.05**	-19 ± 0.8 **-18 ± 3.5**	8 ± 1.2 **0 ± 0**
PH 90H:Chol:Cyst 1:0.98:10	187 ± 18	0.18 ± 0.06	-48 ± 4	16 ± 4	193 ± 27 **226 ± 15**	0.32 ± 0.02 **0.23 ± 0.02**	-33 ± 1.4 **-34 ± 0.5**	5 ± 0.5 **0.8 ±0.11**